Anal. Chem. **2010,** *82,* 1964–1974

Analysis of Opioid and Amyloid Peptides Using Time-of-Flight Secondary Ion Mass Spectrometry

Santiago Solé-Domènech,*,† Björn Johansson,† Martin Schalling,† Jakob Malm,‡ and Peter Sjövall‡

Department of Molecular Medicine and Surgery, Section of Neurogenetics, Karolinska Institutet, SE-171 76 Stockholm, Sweden, and Department of Chemistry and Materials Technology, SP Technical Research Institute of Sweden, P.O. Box 857, SE-50115 Borås, Sweden

The imaging capability and high detection sensitivity of time-of-flight secondary ion mass spectrometry (ToF-SIMS) makes it a potentially attractive complement to other mass spectrometry methods, such as ESI and MALDI, for the analysis of proteins and peptides. We have explored this possibility by performing a systematic analysis of synthetic opioid and amyloid peptides with ToF-SIMS using Bi_3^+ and Au_3^+ primary ions. In the low mass region of the spectra, a number of single amino acid ion peaks were detected, providing information about the amino acid content in each peptide. In the medium and high mass range of the spectra, peaks corresponding to multiple amino acid ions (backbone cleavage ions) as well as molecular ions were detected, allowing for the determination of the amino acid sequence and the molecular mass of the entire peptide, respectively. Detection efficiencies were determined for the molecular ions of some of the peptides, indicating detection limits in the attomole range. The fragmentation patterns observed in the ToF-SIMS analysis of opioid and amyloid peptides showed interesting similarities with collision-induced dissociation (CID) studies using other mass spectrometry methods. The present work provides important progress toward ToF-SIMS proteomics.

Mass spectrometry has been used for several decades to determine the amino acid sequence of peptides and proteins and is still the main technique for this purpose.[1,2] Electrospray ionization (ESI) and matrix-assisted laser desorption ionization (MALDI) are currently the most common ionization methods, but new techniques are continuously being developed.[1,2] In time-of-flight secondary ion mass spectrometry (ToF-SIMS), a beam of high-energy monoatomic or polyatomic primary ions bombard the surface of a solid sample, ejecting charged analyte particles, so-called secondary ions, which are then collected and separated in a ToF analyzer.[3,4] ToF-SIMS has been widely used in materials science for nearly 20 years and has also been proven capable of analyzing biological cells and tissues with an ability to visualize them in situ.[5−8]

Prior to the arrival of cluster ion sources, SIMS analysis of biological substances was primarily performed using monoatomic primary ions.[9−11] In 1976, Benninghoven et al.[10] used an Ar^+ ion source to study more than 40 biologically relevant compounds, including amino acids, peptides, drugs, vitamins, and pharmaceuticals. Emission of highly specific secondary ions was observed from these compounds, such as the $(M + H)^+$ and $(M - H)^-$ molecular ions and related ions, such as $(M - COOH)^+$, in addition to smaller characteristic fragment ions. In 1986, Jabs et al.[11] used ToF-SIMS, also with Ar^+ primary ions, to study apolipoproteins. The apolipoprotein preparation was first digested to generate tryptic peptide fragments, which were then isolated using HPLC and analyzed (at the picomole range) by ToF-SIMS. The results allowed the identification of an apolipoprotein mutant in which arginine was exchanged by histidine. Some other works concerning apolipoprotein structures followed.[12−14] Already then, some of the advantages of ToF-SIMS were pointed out, such as the high accuracy of molecular weight determination (±1 Da) within a mass range up to 3000 Da and the small amount of sample required for the analyses.

Another important advantage of ToF-SIMS in the analysis of peptides is the easy sample preparation and handling. Aubagnac

* Corresponding author. Tel: +46-8-5177 6466. Fax: +46-8-5177 3909. E-mail: santiago.sole@ki.se.

† Karolinska Institutet.

‡ SP Technical Research Institute of Sweden.

(1) Schuchardt, S.; Sickmann, A. *EXS* **2007**, *97*, 141–170.

(2) Canas, B.; Lopez-Ferrer, D.; Ramos-Fernandez, A.; Camafeita, E.; Calvo, E. *Brief. Funct. Genomics Proteomics* **2006**, *4*, 295–320.

(3) Benninghoven, A. *Surf. Sci.* **1994**, *299*, 246–260.

(4) Belu, A. M.; Graham, D. J.; Castner, D. G. *Biomaterials* **2003**, *24*, 3635–3653.

(5) Piehowski, P. D.; Carado, A. J.; Kurczy, M. E.; Ostrowski, S. G.; Heien, M. L.; Winograd, N.; Ewing, A. G. *Anal. Chem.* **2008**, *80*, 8662–8667.

(6) Kim, J. H.; Yu, Y. S.; Kim, D. H.; Lee, T. G.; Moon, D. W.; Kim, K. W. *Biochem. Cell Biol.* **2008**, *86*, 459–467.

(7) Hansson, M.; Grunditz, T.; Isaksson, M.; Jansson, S.; Lausmaa, J.; Molne, J.; Berg, G. *Thyroid* **2008**, *18*, 1215–1220.

(8) Sjovall, P.; Lausmaa, J.; Johansson, B. *Anal. Chem.* **2004**, *76*, 4271–4278.

(9) Benninghoven, A.; Jaspers, D.; Sichtermann, W. *Appl. Phys.* **1976**, *11*, 35–39.

(10) Benninghoven, A.; Sichtermann, W. K. *Anal. Chem.* **1978**, *50*, 1180–1184.

(11) Jabs, H. U.; Assmann, G.; Greifendorf, D.; Benninghoven, A. *J. Lipid Res.* **1986**, *27*, 613–621.

(12) Voneckardstein, A.; Walter, M.; Holz, H.; Benninghoven, A.; Assmann, G.; Roetrige, A.; Kock, R. *J. Lipid Res.* **1991**, *32*, 1465–1476.

(13) Voneckardstein, A.; Funke, H.; Walter, M.; Altland, K.; Benninghoven, A.; Assmann, G. *J. Biol. Chem.* **1990**, *265*, 8610–8617.

(14) Voneckardstein, A.; Funke, H.; Henke, A.; Altland, K.; Benninghoven, A.; Assmann, G. *J. Clin. Invest.* **1989**, *84*, 1722–1730.

10.1021/ac902712f
Published on Web 02/01/2010

et al.[15] used ToF-SIMS to monitor a solid-phase peptide synthesis without any type of sample pretreatment. No chemical treatment was needed to release the growing peptide chains, therefore avoiding cross-contamination and preserving the natural chemical setup. In addition, Sun et al.[16] showed the excellent surface sensitivity, easy sample handling, and low detection limits of ToF-SIMS in the study of the oxidation of methionine-enkephalin, an opioid, in air and under UV irradiation.

ToF-SIMS analysis of peptides and protein films provides valuable information about the amino acid composition of the structures.[17−19] As an example, Canavan et al.[18,20] studied the extracellular matrix (ECM) secreted after cell liftoff using ToF-SIMS operated with Cs^+. Using principal component analysis of the signal intensities from characteristic amino acid secondary ions in the positive spectra, they demonstrated that the major ECM proteins can be identified from their amino acid compositions. However, using only the amino acid ion peaks it was concluded that a specific protein must be present at a relative concentration of at least 10% of the total protein weight in a sample in order to be differentiated from all other proteins using ToF-SIMS,[21] therefore hindering protein characterization. Furthermore, the conformation, orientation, and spatial distribution[20] of protein structures adsorbed onto diverse surfaces have been studied, utilizing the fact that the sampling depth in ToF-SIMS (1−2 nm) is smaller than the size of most proteins.[20] Differences in the observed signal intensities of amino acid fragments on different surfaces were thus associated with conformational variations in the adsorbed proteins, induced by a number of factors, such as denaturation events[22] or charge differences between absorbing surfaces,[23] among others.[24,25] In these studies, the large amounts of data obtained with ToF-SIMS were analyzed using multivariate statistical analysis techniques, such as principal component analysis (PCA), which allows determination of the major differences in amino acid-related peaks of the different data sets.[20]

After the introduction of ToF analyzers, which enormously facilitated data acquisition and provided higher mass resolution and broader mass ranges,[26,27] the arrival of the currently used cluster primary ion sources was an important improvement for ToF-SIMS analysis of peptides, providing enhanced secondary ion yields and detection efficiencies for large characteristic secondary ions.[28] Tempez et al.[29] analyzed several peptide structures and focused on the effect of various large gold cluster primary ions on the peptide fragmentation, secondary ion yields, and damage cross sections. Several amino acid fragment ions (backbone cleavage ions) were detected together with multiple internal cleavage ions and molecular ions. In another study, Cheng et al.[30] performed depth profiling of glassy trehalose thin films doped with peptides using C_{60}^+ ions both for sputtering and analysis. High yields of characteristic secondary ions from trehalose and peptide were observed throughout the film. However, although signal corresponding to the individual amino acids, molecular ions, or multiple amino acid ions could be detected, little attention was paid to how the amino acids were connected to each other (i.e., the peptide sequence). In general, the potential use of ToF-SIMS for amino acid sequencing of peptides and proteins has not, to our knowledge, been thoroughly investigated.

The opioid peptides selected for this study bind to receptors that are found primarily in the central nervous system (CNS) and the gastrointestinal tract. The enkephalins leucine-enkephalin (LE) and methionine-enkephalin-lysine-lysine (MEKK) are pentapeptides localized in nerve endings. Their distribution closely parallels the distribution of opioid receptors, and the peptides are involved in the modulation of the pain response. Similarly, the dynorphins (endorphins) dynorphin A 1−6 (DA 1−6), 1−9 (DA 1−9), and 1−10 (DA 1−10) as well as dynorphin B (DB) are larger polypeptides that possess a potent analgesic activity and are found also in the CNS. The interruption of pain impulses may be mediated by calcium gating via endorphin receptors, enkephalin receptors, or both.[31,32] On the other hand, the amyloid peptides 1−40 and 1−42 are products of APP protein processing by α-secretase and γ-secretase.[33] These peptides and probably related fragments such as amyloid β 1−11 (Aβ 1−11) and 29−40 (Aβ 29−40) accumulate in brain tissue during the pathogenesis of Alzheimer's disease (AD).[34] Even though their exact role during the pathogenesis of the disease is still unclear, they may interfere with synaptic function[34] and trigger the process of hyperphosphorylation of the protein tau (main cause of massive neuronal death in AD) via crosstalk with glycogen synthase kinase 3 (GSK3).[35]

Considering the advantages in the analysis of proteins and peptides, such as the small amount of sample required, easy sample handling, and in situ tissue analysis and imaging, ToF-SIMS may be an interesting complement to ESI/MALDI in some applications of peptide/protein analysis. In this work, we explore this possibility by performing a systematic analysis of synthetic opioid and amyloid peptides with ToF-SIMS using Bi_3^+ and Au_3^+ primary ions. Peaks corresponding to single amino acid ions, multiple amino acid fragment ions, and molecular ions were observed for all peptides, providing information about the

(15) Aubagnac, J. L.; Enjalbal, C.; Drouot, C.; Combarieu, R.; Martinez, J. *J. Mass Spectrom.* **1999**, *34*, 749–754.
(16) Sun, L.; Gardella, J. A., Jr. *Pharm. Res.* **2000**, *17*, 859–862.
(17) Wagner, M. S.; Castner, D. G. *Langmuir* **2001**, *17*, 4649–4660.
(18) Canavan, H. E.; Graham, D. J.; Cheng, X.; Ratner, B. D.; Castner, D. G. *Langmuir* **2007**, *23*, 50–56.
(19) Lhoest, J. B.; Wagner, M. S.; Tidwell, C. D.; Castner, D. G. *J. Biomed. Mater. Res.* **2001**, *57*, 432–440.
(20) Michel, R.; Castner, D. G. *Surf. Interface Anal.* **2006**, *38*, 1386–1392.
(21) Wagner, M. S.; Horbett, T. A.; Castner, D. G. *Langmuir* **2003**, *19*, 1708–1715.
(22) Michel, R.; Pasche, S.; Textor, M.; Castner, D. G. *Langmuir* **2005**, *21*, 12327–12332.
(23) Wang, H.; Castner, D. G.; Ratner, B. D.; Jiang, S. Y. *Langmuir* **2004**, *20*, 1877–1887.
(24) Henry, M.; Dupont-Gillain, C.; Bertrand, P. *Langmuir* **2003**, *19*, 6271–6276.
(25) Lhoest, J. B.; Detrait, E.; van den Bosch de Aguilar, P.; Bertrand, P. *J.Biomed. Mater. Res.* **1998**, *41*, 95–103.
(26) Niehuis, E.; Heller, T.; Feld, H.; Benninghoven, A. *J. Vac. Sci. Technol. A-Vac. Surf. Films* **1987**, *5*, 1243–1246.
(27) Schueler, B. W. *Microsc. Microanal. Microstruct.* **1992**, *3*, 119–139.
(28) Kollmer, F. *Appl. Surf. Sci.* **2004**, *203*, 153–158.
(29) Tempez, A.; Schultz, J. A.; Della-Negra, S.; Depauw, J.; Jacquet, D.; Novikov, A.; Lebeyec, Y.; Pautrat, M.; Caroff, M.; Ugarov, M.; Bensaoula, H.; Gonin, M.; Fuhrer, K.; Woods, A. *Rapid Commun. Mass Spectrom.* **2004**, *18*, 371–376.
(30) Cheng, J.; Winograd, N. *Anal. Chem.* **2005**, *77*, 3651–3659.
(31) Jacob, L. S. *Pharmacology*, 4th ed.; Lippincot Williams & Wilkins: New York, 1996.
(32) Bodnar, R. J. *Peptides* **2008**, *29*, 2292–2375.
(33) Mattson, M. P. *Nature* **2004**, *430*, 631–639.
(34) Nimmrich, V.; Ebert, U. *Rev. Neurosci.* **2009**, *20*, 1–12.
(35) Hooper, C.; Killick, R.; Lovestone, S. *J. Neurochem.* **2008**, *104*, 1433–1439.

Table 1. List of Peptides Analyzed in the Study

peptide name	sequence (one-letter code)	no. of residues	mass (Da)	purity (%)	conc (mg/mL)
leucine-enkephalin	YGGFL	5	555.27	98.1	1.0
dynorphin A 1−6	YGGFLR	6	711.37	99.2	3.3
methionine-enkephalin-lysine-lysine	YGGFMKK	7	829.42	96.0	1.0
amyloid β 29−40	GAIIGLMVGGVV	12	1084.63	95.9	2.0
dynorphin A 1−9	YGGFLRRIR	9	1136.66	98.9	2.0
dynorphin A 1−10	YGGFLRRIRP	10	1233.71	99.0	1.0
amyloid β 1−11	DAEFRHDSGYE	11	1324.53	98.0	2.0
dynorphin B	YGGFLRRQFKVVT	13	1569.88	97.0	1.0

amino acid composition, amino acid sequence, and molecular weight, respectively. Furthermore, detection efficiencies were determined for some of the peptides, providing information about detection limits that can be expected in, for example, tissue samples (where, however, matrix effects must be considered). The set of selected peptides covers a wide range of molecular masses and residue compositions, allowing analysis of the effects of the molecular weight and the specific amino acid composition on the fragmentation process and secondary ion yields. The enkephalins and the dynorphins have similar sequences but mainly differ by the presence of the basic amino acid residue arginine that may influence the fragmentation process significantly, due to its nucleophilicity.[36] The analysis of amyloid peptides is interesting also due to their hydrophobic nature, proven to strongly impair the ionization process.[37]

EXPERIMENTAL SECTION

Peptide Preparations. The eight different peptides that were analyzed with ToF-SIMS, six endogenous opioids and two separate fragments of amyloid β, are listed together with their molecular weights and amino acid sequences in Table 1. The peptides were provided in pure crystal form by Bachem (Bubendorf, Switzerland).

Each peptide sample was introduced into a sterilized Eppendorf tube and dissolved in Milli-Q water without further purification at concentrations given in Table 1. The resulting solutions were vortexed several minutes to ensure complete dissolution of the peptide. A 5−10 μL drop of the peptide solution was deposited onto the surface of a silicon wafer substrate and allowed to dry at room temperature, leaving a peptide deposit coating the surface. The wafers were previously cleaned by washing sequentially in heptane, acetone, and ethanol. After preparation, the samples were introduced into the vacuum chamber of the ToF-SIMS instrument for analysis of the pure peptide deposits.

ToF-SIMS Analysis. The ToF-SIMS analysis was carried out using a ToF-SIMS IV instrument (ION-TOF GmbH, Münster, Germany) equipped with a reflectron-type time-of-flight mass spectrometer. Aβ 29−40 and DB were analyzed using 25 keV Au_3^+ primary ions, while 25 keV Bi_3^+ was used for the other six peptides. The ToF-SIMS spectrometer was initially equipped with a gold ion source, which was then replaced by a bismuth source due to technical considerations. Since both bismuth and gold clusters proved well-suited for peptide analysis, we find it appropriate to include data with both sources in the present paper. Indeed, the spectra using Au_3^+ primary ions were found to be qualitatively similar to the spectra obtained using Bi_3^+ primary ions, with regard to observations of the different types of secondary ions and the approximate magnitude of their yields. However, no quantitative comparisons are made between spectra obtained using different primary ion species. The data were acquired using low-energy electron flooding for charge compensation and with the instrument optimized for high mass resolution (bunched mode, mass resolution $m/\Delta m$ ~5000, lateral resolution 3−5 μm). The pulsed primary ion current was 0.1 pA for Bi_3^+ and 0.03/0.04 pA for Au_3^+. During acquisition, the primary ion beam was scanned over an analysis area of 100 × 100 μm^2 or 200 × 200 μm^2, collecting separate spectra from 128 × 128 raster points. The acquisition time was 100 s (Bi_3^+) or 400 s (Au_3^+), giving a maximum accumulated primary ion dose density below 1×10^{12} ions/cm^2. In order to obtain the detection efficiencies (see below), the disappearance cross sections were determined for five peptides (using Bi_3^+ primary ions) from the decay in the recorded signal during longer acquisition time (600 s, 100 × 100 μm^2 analysis area).

Calibration, Peak Assignments and Data Analysis. The increased useful mass range from use of cluster primary ions allows analysis of biosubstances of higher molecular mass, but masses are thus often calculated from flight times by extrapolation. In the literature about mass spectrometry in general[38] and ToF-SIMS[39,40] it is often said that interpolation is inherently more accurate than extrapolation. This is in agreement with our experience from ToF-SIMS analysis of biomedical samples. Therefore, calibration of the recorded spectra was carried out including the molecular ions as well as some ions at the low mass range—CH_3, C_2H_2, C_3H_2, C_4H_2 for the positive and C, C_2, C_3, C_4H for the negative ion spectra—in order to cover a wide range of masses and allowing the assignment of peaks by interpolation. For all peptides, reliable signals from $(M + H)^+$ and $(M - H)^-$ molecular ions were observed and included in the calibration procedure. Assignments were slightly less ambiguous after including the molecular ions in the calibration. However, it should be noted that this procedure can only be applied when a safe assignment of the molecular peak can be made, such as in the present case when pure samples of known

(36) Hoffmann, E., Stroobant, V. *Mass Spectrometry: Principles and Applications*, 2nd ed.; John Wiley & Sons: Chichester, 2002.
(37) Mirza, S. P.; Halligan, B. D.; Greene, A. S.; Olivier, M. *Physiol. Genomics* **2007**, *30*, 89–94.
(38) Webb, K.; Bristow, T.; Sargent, M.; Stein, B. *Methodology for Accurate Mass Measurement of Small Molecules. Best Practice Guide*; LGC Limited: Teddington, 2004.
(39) *CasaXPS: Processing software for XPS, AES, SIMS and more*; Casa Software Ltd, 2007. Available at www.casaxps.com.
(40) Green, F. M.; Gilmore, I. S.; Seah, M. P. *J. Am. Soc. Mass Spectrom.* **2006**, *17*, 514–523.

peptides were analyzed, and may not be possible to use in the analysis of, for example, unknown peptide mixtures.

Peaks were assigned and included in the data set only when the corresponding assignment provided a relative mass accuracy of -100 ppm $< W <$100 ppm, otherwise the peak was discarded. The relative mass accuracy W is given by

$$W = \frac{\Delta M}{M}$$

where ΔM is the mass accuracy and M is the theoretical mass value for a specific peak. The mass accuracy ΔM is the difference between the monoisotopic mass of the peak measured by the analyst (M_P) and the predicted monoisotopic mass value M_T'

$$\Delta M = M_P - M_T'$$

Only the monoisotopic peaks were used to record signal intensities. However, in the case of interferences with higher isotopes from other ions, the signal intensity was corrected for the contribution from the interfering isotope when this contribution was larger than 5% (as calculated from the isotopic distribution of the interfering ion). In the case of unknown peptide mixture samples, such a correction procedure may not be applicable due to difficulties in the assignment of the interfering peaks. However, several approaches for this problem are already in use in software packages for the interpretation of proteomic data (as an example, see Breen et al.[41]) and could possibly be adapted for use with ToF-SIMS.

Theoretical peptide fragments for both positive and negative spectra were calculated using the software applications Protein Prospector (UCSF Mass Spectrometry Facility, prospector.ucsf.edu) and GPMAW (General Protein/Mass Analysis for Windows, Lighthouse Data).

The recorded secondary ion signal intensities are presented as secondary ion yields

$$Y(X_i^{q+}) = \frac{N(X_i^{q+})}{N_{PI}}$$

where $Y(X_i^{q+})$ is the secondary ion yield of a specific secondary ion X_i^{q+}, $N(X_i^{q+})$ is the number of detected secondary ions (measured under static conditions), and N_{PI} is the number of applied primary ions.[28,42] Due to the sputtering and the molecular damage caused by the primary ion impact, the number of sample molecules on the surface is gradually reduced during analysis, resulting in an exponential decay in the rate of the secondary ion detection

$$\frac{dN(X_i^{q+})}{dt} = \left(\frac{dN(X_i^{q+})}{dt}\right)_{t=0} e^{-\sigma(X_i^{q+})PIDD}$$

where PIDD is the accumulated primary ion dose density at time t and $[dN(X_i^{q+})/dt]_{t=0}$ is the rate of detection at the start of the acquisition. The disappearance cross section $\sigma(X_i^{q+})$ is obtained from the slope of the exponential decay and corresponds to the mean area from which no further ion X_i^{q+} can be generated per primary ion impact. The efficiency E represents the maximum number of secondary ions that can be detected per unit surface area, i.e., when all the sample molecules have been consumed during analysis

$$E(X_i^{q+}) = \frac{Y(X_i^{q+})}{\sigma(X_i^{q+})}$$

Finally, detection limits $D(X_i^{q+})$, defined as the number of sample molecules required to obtain a significant signal, were calculated as

$$D(X_i^{q+}) = \frac{nC_{surf}}{E(X_i^{q+})}$$

where n is the number of secondary ions required for obtaining a significant signal and C_{surf} is the surface concentration of the analyzed molecule. In our calculation below we assumed $n =$ 10 and $C_{surf} = 1.4 \times 10^{18}$ molecules/m^2, which is a typical value of the surface concentration of lipid molecules in a membrane leaflet.[43] In order to use the obtained values as guidelines for detection limits in other types of samples, matrix effects must be taken into account.

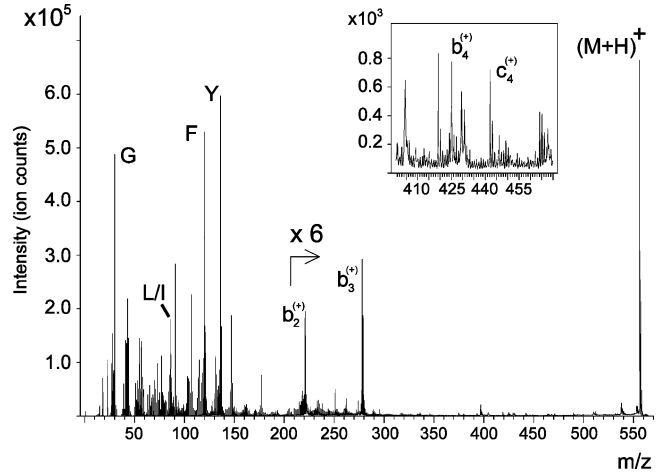

Figure 1. Positive ToF-SIMS spectrum of leucine-enkephalin (YGGFL). Peaks corresponding to amino acid specific immonium ions (G, L/I, F and Y), multiple amino acid backbone cleavage fragment ions ($b_2^{(+)}$, $b_3^{(+)}$, $b_4^{(+)}$, $c_4^{(+)}$), and the molecular ion (M + H$^+$) are highlighted.

RESULTS AND DISCUSSION

The selection of peptides was based on the following three basic principles: (1) provide variation in the number of amino acids (between 5 and 13) and molecular weight (between 500 and 1600 Da) of the peptides, in order to study the effect of peptide size on the fragmentation of the structures. (2) All opioids contain the basic root sequence YGGFL (LE) but vary by the presence of additional specific amino acids such as arginine (R) (in YGGFLR and YGGFLRRIR) and lysine (K) (in YGGFMK), known to be of

(41) Breen, E. J.; Holstein, W. L.; Hopwood, F. G.; Smith, P. E.; Thomas, M. L.; Wilkins, M. R. *Spectroscopy* **2003**, *17*, 579–595.

(42) Touboul, D.; Kollmer, F.; Niehuis, E.; Brunelle, A.; Laprevote, O. *J. Am. Soc. Mass Spectrom.* **2005**, *16*, 1608–1618.

(43) Prinz, C.; Hook, F.; Malm, J.; Sjovall, P. *Langmuir* **2007**, *23*, 8035–8041.

Table 2. Major Immonium and Related Ions Described in the Literature and Detected in ToF-SIMS Spectra

name	amino acid	related ion[a]	species	monoisotopic mass
glycine	G	G ii	CH_4N^+	30.0344
valine	V	V ii	$C_4H_{10}N^+$	72.0813
threonine	T	T ii	$C_3H_8NO^+$	74.0606
leucine-isoleucine	L/I	L/I ii	$C_5H_{12}N^+$	86.0970
aspartic acid	D	D ii	$C_3H_6NO_2^+$	88.0399
lysine-glutamine	K/Q	K r1/Q r1	$C_5H_{10}N^+$	84.0813
glutamic acid	E	E ii	$C_4H_8NO_2^+$	102.0555
methionine	M	M r1	$C_2H_5S^+$	61.0112
histidine	H	H ii	$C_5H_8N_3^+$	110.0718
		H r1	$C_4H_6N_2^+$	82.0531
phenylalanine	F	F ii	$C_8H_{10}N^+$	120.0813
arginine - proline	R/P	R r1/P r1	$C_4H_8N^+$	70.0657
arginine	R	R r2	$C_4H_{11}N_2^+$	87.0922
		R r3	$CH_3N_2^+$	43.0296
		R r4	$CH_5N_3^+$	59.0483
		R r5	$C_2H_7N_3^+$	73.0640
tyrosine	Y	Y ii	$C_8H_{10}NO^+$	136.0762
		Y r1	$C_3H_3O^+$	55.0184

[a] "ii" stands for immonium ion, while "r" stands for related ion.

basic nature, and proline (P) (in YGGFLRRIRP), suggested to increase the formation of $c_n^{(-)}$ ions, one of the most abundant ion types in negative ion spectra.[44] This selection of peptides allows for the study of the effect of these residues in the fragmentation of the structures. (3) The biological origin and physiological role of these peptides will be of use in future experiments focusing on the study of AD mouse brain tissue.

Figure 1 shows an example of a positive mass spectrum from a peptide using ToF-SIMS. The spectrum covers the mass range from 0 to m/z 600, which is above the molecular weight of the analyzed peptide (LE). In the low-mass region, the spectrum shows a large number of high-intensity peaks corresponding to low-mass fragment ions. Some of these peaks are characteristic for specific amino acids contained in the peptide, including tyrosine (Y), glycine (G), leucine (L), and phenylalanine (F), and are often referred to as immonium ions in collision-induced dissociation studies (CID).[36,45,46] These ions provide information about the amino acid composition of the peptide and have the general structure $H_2N^+{=}HC{-}R$ where R is the side chain group of the specific amino acid, formed after internal cleavage of the peptide bonds at the N and C terminal sites. In the high-mass region, a strong peak is observed at m/z 556.28, which corresponds to the protonated molecular ion of LE, $(M + H)^+$. In the intermediate mass region, m/z 150−500, fragments containing multiple amino acid residues arising from cleavage of the peptide backbone skeleton[36,45,47] are shown ($b_2^{(+)}$, $b_3^{(+)}$, and $b_4^{(+)}$ $c_4^{(+)}$ in Figure 1). Mass differences between these ion peaks correspond to specific amino acid residue losses and therefore provide information about the amino acid sequence in the peptide. The spectra (positive and negative ion) from all studied peptides showed the same principal features described here. The information provided by these three different types of secondary ions, (i) single amino acid fragments, (ii) molecular ions, and (iii) multiple amino acid fragments, are described separately in detail below.

Compared to previous ToF-SIMS studies of proteins and peptides using monoatomic primary ions (Ar^+,[10] Cs^+,[18–20] and Ga^+ [48]), the spectra obtained in the present study using Au_3^+ and Bi_3^+ cluster primary ions show significantly higher yields for secondary ions in the mass range >100 Da, allowing for a more detailed analysis of, in particular, molecular ions and multiple amino acid fragment ions. In general, spectra obtained using monoatomic sources have shown primarily single amino acid fragment ions and molecular ions, whereas multiple amino acid fragment ions in the middle mass range have not been previously described in detail.

Single Amino Acid Fragments (Immonium Ions). Table 2 shows a list of the major immonium and related ions that have been described in previous studies on peptides and proteins.[18,49] For each amino acid, the one-letter notation is provided together with the chemical formula and the monoisotopic mass of the respective immonium ion.

In Figure 2, the secondary ion yields for the different immonium ions are shown for each peptide, as measured from the recorded spectra. For all peptides, significant signal is observed from the immonium ions that correspond to amino acids contained in the peptide, while peaks from amino acids not contained in the peptide show no or very low signal. All peptides show similar features. Comparing the different immonium peaks, the ions produced by R and F show high yields for all peptides. This is similar to CID, where the observation has been assigned to the apparent stability given by favorable resonance effects and/or inductive effects coming from alkyl side chain groups.[36] In addition, aspartic acid (D) and glutamic acid (E) show low intensities, probably due to the electron-withdrawing effect carried out by the carboxyl group that destabilizes the positive ion. The secondary ion yields for Y and L ions differ substantially among the peptides, as do the yields for K and threonine (T) ions, when formed. The amino acids R and methionine (M) can be identified by related ions such as $C_4H_8N^+$ (70.0657 Da) or $C_2H_5S^+$ (61.0112 Da), as reported in previous studies.[18,49] All R-related ions follow

(44) Harrison, A. G.; Young, A. B. *J. Mass Spectrom.* **2005**, *40*, 1173–1186.
(45) Biemann, K.; Martin, S. A. *Mass Spectrom. Rev.* **1987**, *6*, 1–75.
(46) Falick, A. M.; Hines, W. M.; Medzihradszky, K. F.; Baldwin, M. A.; Gibson, B. W. *J. Am. Soc. Mass Spectrom.* **1993**, *4*, 882–893.
(47) Harrison, A. G. *J. Am. Soc. Mass Spectrom.* **2001**, *12*, 1–13.
(48) Maux, D.; Enjalbal, C.; Martinez, J.; Aubagnac, J. L. *J. Am. Soc. Mass Spectrom.* **2001**, *12*, 1099–1105.
(49) Mantus, D. S.; Ratner, B. D.; Carlson, B. A.; Moulder, J. F. *Anal. Chem.* **1993**, *65*, 1431–1438.

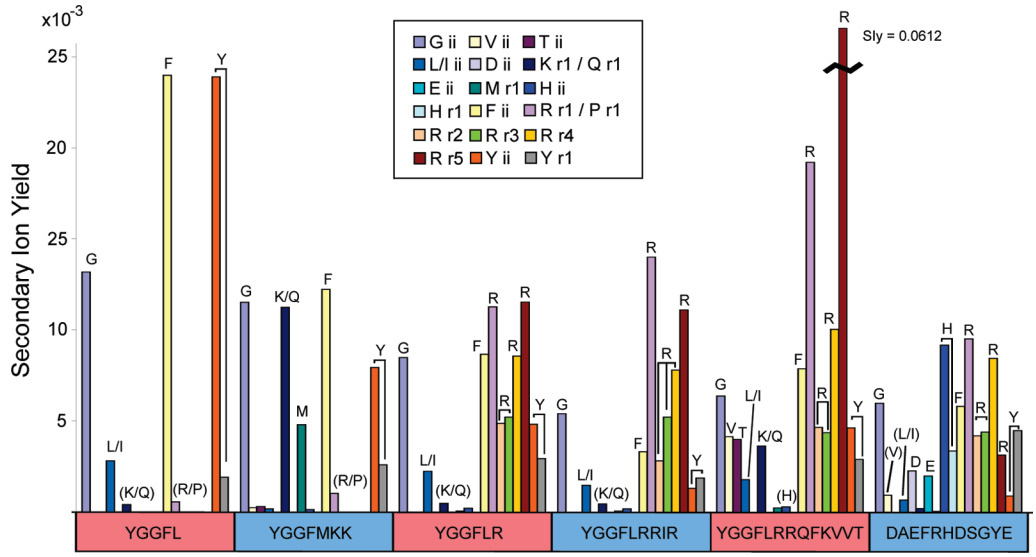

Figure 2. Measured secondary ion yields for immonium ions observed in positive spectra from all peptides. Letters "ii" stand for "immonium ion" and "r" stands for "related ion.

Table 3. Positive and Negative Molecular Ions of All Eight Peptides[a]

peptide	chemical formula	observed mass (Da)	primary ion	SI yield (SI/PI)	efficiency (SI/m^3)	detection limit (mol)
YGGFL	$C_{28}H_{38}N_5O_7^+$	556.28	Bi_3^+	2.29×10^{-3}	3.96×10^{13}	5.9×10^{-19}
	$C_{28}H_{36}N_5O_7^-$	554.26	Bi_3^+	6.75×10^{-3}	1.54×10^{14}	1.5×10^{-19}
YGGFLR	$C_{34}H_{50}N_9O_8^+$	712.38	Bi_3^+	2.29×10^{-3}	4.10×10^{13}	5.7×10^{-19}
	$C_{34}H_{48}N_9O_8^-$	710.36	Bi_3^+	1.74×10^{-3}	3.14×10^{13}	7.4×10^{-19}
YGGFMKK	$C_{39}H_{60}N_9O_9S^+$	830.43	Bi_3^+	3.17×10^{-4}	4.09×10^{12}	5.7×10^{-18}
	$C_{39}H_{58}N_9O_9S^-$	828.41	Bi_3^+	5.82×10^{-4}	9.52×10^{12}	2.4×10^{-18}
GAIIGLMVGGVV	$C_{49}H_{89}N_{12}O_{13}S^+$	1085.64	Au_3^+	1.14×10^{-5}		
	$C_{49}H_{87}N_{12}O_{13}S^-$	1083.63	Au_3^+	3.66×10^{-4}		
YGGFLRRIR	$C_{52}H_{85}N_{18}O_{11}^+$	1137.67	Bi_3^+	7.37×10^{-5}	1.31×10^{12}	1.8×10^{-17}
	$C_{52}H_{83}N_{18}O_{11}^-$	1135.65	Bi_3^+	1.64×10^{-4}		
YGGFLRRIRP	$C_{57}H_{92}N_{19}O_{12}^+$	1234.73	Bi_3^+	3.86×10^{-5}		
	$C_{57}H_{90}N_{19}O_{12}^-$	1232.70	Bi_3^+	4.96×10^{-5}		
DAEFRHDSGYE	$C_{56}H_{77}N_{16}O_{22}^+$	1325.55	Bi_3^+	3.64×10^{-5}		
	$C_{56}H_{75}N_{16}O_{22}^-$	1323.53	Bi_3^+	4.68×10^{-6}	8.50×10^{10}	2.7×10^{-16}
YGGFLRRQFKVVT	$C_{74}H_{116}N_{21}O_{17}^+$	1570.88	Au_3^+	5.76×10^{-5}		
	$C_{74}H_{114}N_{21}O_{17}^-$	1568.89	Au_3^+	2.27×10^{-5}		

[a] Chemical formula, assigned mass, and yields are shown.

similar secondary yield patterns (with minor differences) in all R-containing peptides.

Although the observation of immonium peaks indicate the presence of the corresponding amino acids in the peptide, their signal intensities are not proportional to the abundance of the amino acid in the peptide structure, suggesting that quantitative information about the amino acid composition cannot be directly obtained from the immonium ion signal intensities. Rather, the signal intensity distribution between the different immonium peaks may be used as a fingerprint for the specific peptide. Taken together, these observations demonstrate that the ToF-SIMS spectra can provide information about the amino acids contained in the peptide.

Molecular Ions. Strong signal intensities were observed from molecular ions both in the positive, $(M + H)^+$, and negative, $(M - H)^-$, ion modes for all analyzed peptides. The measured secondary ion yields of the molecular ions are listed in Table 3, together with their chemical composition and peak masses. In addition, disappearance cross sections were obtained for some peptides from the signal intensity decay in measurements carried out over extended analysis. Efficiencies calculated from the measured secondary ion yields and disappearance cross sections are also provided. The efficiencies provide the maximum number of secondary ions that can be detected per unit area on the sample surface. The detection limits listed in Table 3 were calculated from the efficiencies and represent the minimum amount of sample molecules needed to obtain a significant signal. For this calculation, 10 detected secondary ions was considered to be a significant signal and the surface concentration of peptide molecules was taken to be the same as the surface concentration of phosphatidylcholine molecules (roughly the same molecular weight as the analyzed peptides) in a single leaflet of a membrane bilayer.[43] The results indicate that peptide amounts in the attomole regime can be detected using the molecular ion peak. In addition, the positive and negative molecular ions for Aβ 1−11 and Aβ 29−40 were easily detected in the spectra. These peptides are generally difficult to analyze with conventional mass spectroscopy due to their hydrophobicity[37] and often require the use of special ionization methods.

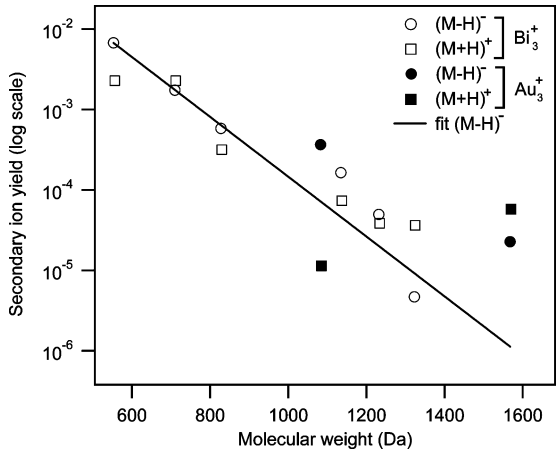

Figure 3. Measured secondary ion yields for the molecular ions of all peptides, plotted as a function of molecular weight. The solid line is an exponential fit made to the data representing negative molecular ions obtained from spectra using Bi_3^+ primary ions.

Figure 3 shows the secondary ion yields of the negative and positive molecular ions as a function of ion mass. The secondary ion yields were found to decrease with increasing ion mass, approximately following an exponential decay. This decay is consistent with previous studies in which similar observations were assigned to a lower desorption yield and an increase in metastability for high weight molecules in ToF-SIMS.[50]

Multiple Amino Acid Fragments. The following analysis of multiple amino acid fragments was performed only for the opioid peptides, for which a number of such fragments were observed and consistently assigned. In contrast, the abundance of multiple amino acid fragment ions in the spectra from the amyloid peptides was found to be too low to admit similar analysis.

Multiple amino acid fragment ions, or so-called backbone cleavage ions, have been studied in detail using CID,[45,47,51] where they have been categorized according to the cleavage position in the peptide backbone. The most abundant of these fragment ions are those in which only one backbone bond is cleaved, i.e., fragment ions containing either the C-terminal or the N-terminal side of the peptide, while fragment ions requiring two cleavage positions (internal fragments) are less abundant. The structure and notations of the most abundant multiple amino acid fragment ions are shown schematically in Figure 4. Each of these fragments contains a positive or negative charge that is held either by the C-terminal or the N-terminal side of the fragment. The cleavage of the peptide backbone at the C−C bond of the $-C_\alpha(R)-C(=O)-$ unit (where R is the amino acid side chain) produces ions that are named a_n and x_n, depending on whether the ion charge is held by the N or the C-terminal side of the

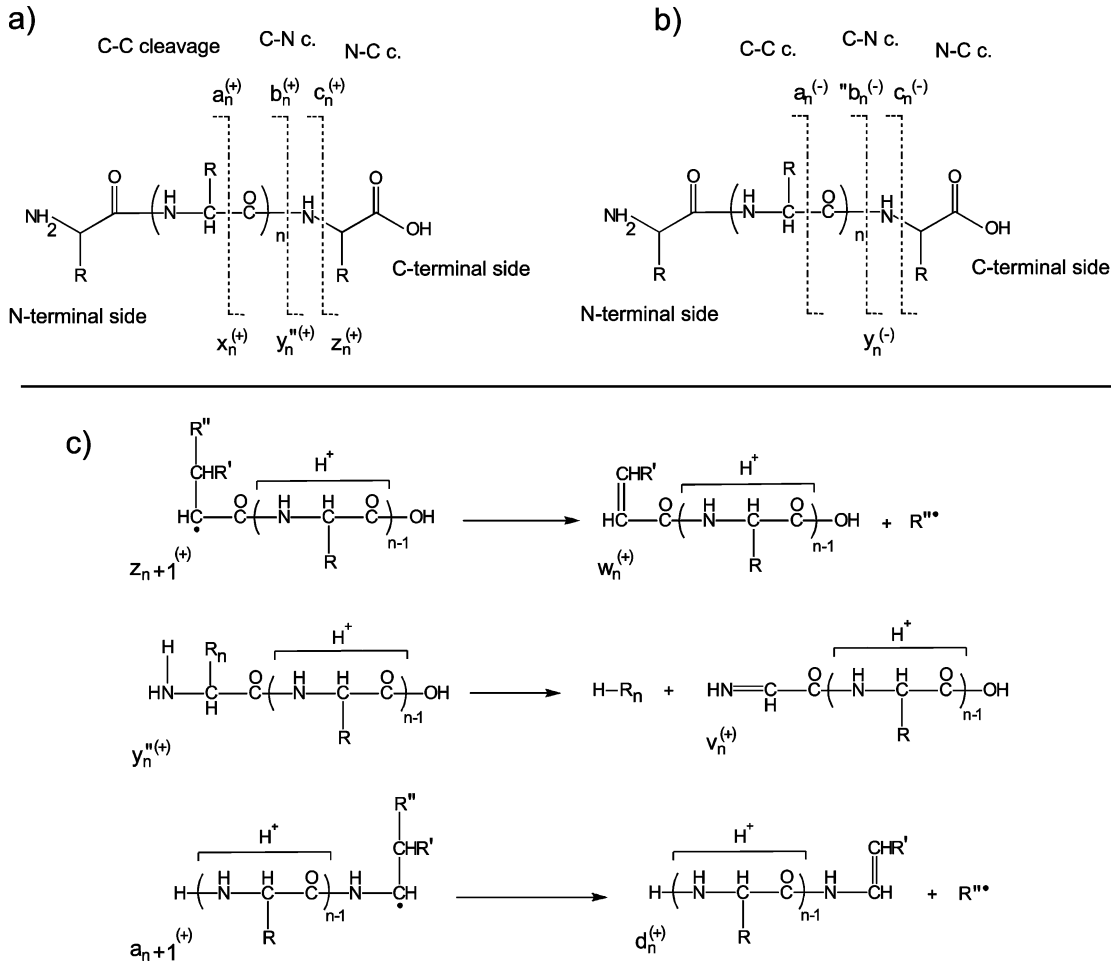

Figure 4. Schematic figure showing the cleavage positions and corresponding notations of the different categories of peptide backbone cleavage fragment ions. (a) Positive backbone cleavage ions, (b) negative backbone cleavage ions, and (c) side chain cleavage ions. R refers to the amino acid side chain.

Table 4. Positive and Negative Backbone and Side Chain Cleavage Ions for Dynorphin A 1-6[a]

ion	species	observed mass (Da)	deviation W (ppm)	SI yield
$a_2^{(+)}$	$C_{10}H_{13}N_2O_2^+$	193.10	0,5	3.45×10^{-5}
$a_3^{(+)}$	$C_{12}H_{16}N_3O_3^+$	250.08	−135,1	–
$a_4^{(+)}$	$C_{21}H_{25}N_4O_4^+$	397.02	−414,9	–
$a_5^{(+)}$	$C_{27}H_{36}N_5O_5^+$	510.26	−22,9	2.94×10^{-6}
$b_2^{(+)}$	$C_{11}H_{13}N_2O_3^+$	221.12	122,6	–
$b_3^{(+)}$	$C_{13}H_{16}N_3O_4^+$	278.10	−33,4	5.61×10^{-5}
$b_4^{(+)}$	$C_{22}H_{25}N_4O_5^+$	425.20	40,5	2.06×10^{-6}
$b_5^{(+)}$	$C_{28}H_{36}N_5O_6^+$	–	–	–
$c_2^{(+)}$	$C_{11}H_{16}N_3O_3^+$	238.12	1,7	9.88×10^{-6}
$c_3^{(+)}$	$C_{13}H_{19}N_4O_4^+$	295.16	61,0	8.52×10^{-6}
$c_4^{(+)}$	$C_{22}H_{28}N_5O_5^+$	442.23	44,1	2.44×10^{-6}
$c_5^{(+)}$	$C_{28}H_{39}N_6O_6^+$	555.30	1,6	2.26×10^{-6}
$x_1^{(+)}$	$C_7H_{13}N_4O_3^+$	201.10	−7,5	3.41×10^{-4}
$x_2^{(+)}$	$C_{13}H_{24}N_5O_4^+$	314.19	13,7	5.03×10^{-5}
$x_3^{(+)}$	$C_{22}H_{33}N_6O_5^+$	461.23	−27,3	2.09×10^{-5}
$x_4^{(+)}$	$C_{24}H_{36}N_7O_7^+$	518.26	−14,3	1.59×10^{-5}
$x_5^{(+)}$	$C_{26}H_{39}N_8O_7^+$	575.29	−7,0	9.25×10^{-6}
$y_1''^{(+)}$	$C_6H_{15}N_4O_2^+$	175.12	33,1	3.34×10^{-4}
$y_2''^{(+)}$	$C_{12}H_{26}N_5O_3^+$	288.20	−4,2	4.96×10^{-5}
$y_3''^{(+)}$	$C_{21}H_{35}N_6O_4^+$	435.26	−23,0	1.11×10^{-5}
$y_4''^{(+)}$	$C_{23}H_{38}N_7O_5^+$	492.29	−13,6	2.18×10^{-5}
$y_5''^{(+)}$	$C_{25}H_{41}N_8O_6^+$	549.31	−8,2	2.18×10^{-5}
$z_1{+}1^{(+)}$	$C_6H_{13}N_3O_2^+$	159.11	39,6	2.27×10^{-4}
$z_2{+}1^{(+)}$	$C_{12}H_{24}N_4O_3^+$	272.17	−45,9	1.53×10^{-5}
$z_3{+}1^{(+)}$	$C_{21}H_{33}N_5O_4^+$	419.25	−5,0	3.89×10^{-6}
$z_4{+}1^{(+)}$	$C_{23}H_{36}N_6O_5^+$	476.26	−21,8	3.36×10^{-6}
$z_5{+}1^{(+)}$	$C_{25}H_{39}N_7O_6^+$	533.26	−64,1	2.75×10^{-6}
$w_2^{(+)}$	$C_9H_{17}N_4O_3^+$	229.13	−3,9	1.14×10^{-3}
$v_2^{(+)}$	$C_8H_{16}N_5O_3^+$	230.13	22,6	1.39×10^{-4}
$v_3^{(+)}$	$C_{14}H_{27}N_6O_4^+$	343.20	−12,8	9.18×10^{-5}
$v_6^{(+)}$	$C_{27}H_{42}N_9O_7^+$	604.31	−14,4	3.02×10^{-5}
$a_1^{(-)}$	$C_8H_{10}NO^-$	136.08	13,2	2.53×10^{-5}
$a_2^{(-)}$	$C_{10}H_{13}N_2O_2^-$	193.07	−131,5	–
$a_3^{(-)}$	$C_{12}H_{16}N_3O_3^-$	250.09	−104,4	–
$a_4^{(-)}$	$C_{21}H_{25}N_4O_4^-$	397.16	−59,9	3.79×10^{-6}
$a_5^{(-)}$	$C_{27}H_{36}N_5O_5^-$	510.25	−40,5	2.37×10^{-6}
$a_6^{(-)}$	$C_{33}H_{48}N_9O_6^-$	666.32	−81,6	1.24×10^{-5}
$''b_2^{(-)}$	$C_{11}H_{11}N_2O_3^-$	219.09	53,4	2.24×10^{-5}
$''b_3^{(-)}$	$C_{13}H_{14}N_3O_4^-$	276.12	61,2	7.91×10^{-6}
$''b_4^{(-)}$	$C_{22}H_{23}N_4O_5^-$	–	–	–
$''b_5^{(-)}$	$C_{28}H_{34}N_5O_6^-$	536.37	225,6	–
$c_1^{(-)}$	$C_9H_{11}N_2O_2^-$	179.10	107,2	–
$c_2^{(-)}$	$C_{11}H_{14}N_3O_3^-$	236.12	69,5	1.02×10^{-4}
$c_3^{(-)}$	$C_{13}H_{17}N_4O_4^-$	293.14	65,8	9.76×10^{-5}
$c_4^{(-)}$	$C_{22}H_{26}N_5O_5^-$	440.20	7,5	1.45×10^{-5}
$c_5^{(-)}$	$C_{28}H_{37}N_6O_6^-$	553.27	−8,3	6.25×10^{-6}
$y_1^{(-)}$	$C_6H_{13}N_4O_2^-$	173.12	98,2	1.41×10^{-4}
$y_2^{(-)}$	$C_{12}H_{24}N_5O_3^-$	286.20	36,3	3.31×10^{-5}
$y_3^{(-)}$	$C_{21}H_{33}N_6O_4^-$	433.26	5,3	1.74×10^{-5}
$y_4^{(-)}$	$C_{23}H_{36}N_7O_5^-$	490.27	−6,9	1.08×10^{-5}
$y_5^{(-)}$	$C_{25}H_{39}N_8O_6^-$	547.29	−12,8	2.49×10^{-5}

[a] Chemical formula, assigned masses, assignment deviations (W), and yields are shown.

fragment, respectively. Similarly, cleavage of the peptide backbone at the C−N bond of the −(O=)C−N(−H)− unit gives rise to ions named b_n and y_n, whereas cleavage of the peptide at the N−C bond of the −N(H)−C_α(R)− unit produces ions named c_n and z_n ions. Additionally, and for positive ions only, we have observed fragments originating from the cleavage of the side chain of the amino acid residues, giving rise to ions named v_n and w_n, when the charge is held by the C-terminal side of the fragment, and d_n ions, if the charge is held by the N-terminal side. Negative ions $y_n^{(-)}$ and $''b_n^{(-)}$ have two less protons than the analogous positive $y_n''^{(+)}$ and $b_n^{(+)}$ ions, respectively, whereas $a_n^{(-)}$ and $c_n^{(-)}$ ions are analogous to $a_n^{(+)}$ and $c_n^{(+)}$ ions.[47,51]

As a representative example, Table 4 shows all backbone and side chain cleavage ions observed in positive and negative ToF-SIMS spectra of DA 1−6. Chemical formulas for the ions, monoisotopic masses, deviation of the assignments, and secondary ion yields are given.

Figure 5a shows a positive spectrum of DA 1−6, in which all $y_n''^{(+)}$ ions as well as a number of $x_n^{(+)}$ and $z_n^{(+)}$ ions can be observed. For most of the studied opioid peptides, these ions show high abundances, and the shapes of the corresponding peaks are well-defined, making reliable peak assignments

(50) Touboul, D.; Halgand, F.; Brunelle, A.; Kersting, R.; Tallarek, E.; Hagenhoff, B.; Laprevote, O. *Anal. Chem.* **2004**, *76*, 1550–1559.

(51) Harrison, A. G. *J. Am. Soc. Mass Spectrom.* **2002**, *13*, 1242–1249.

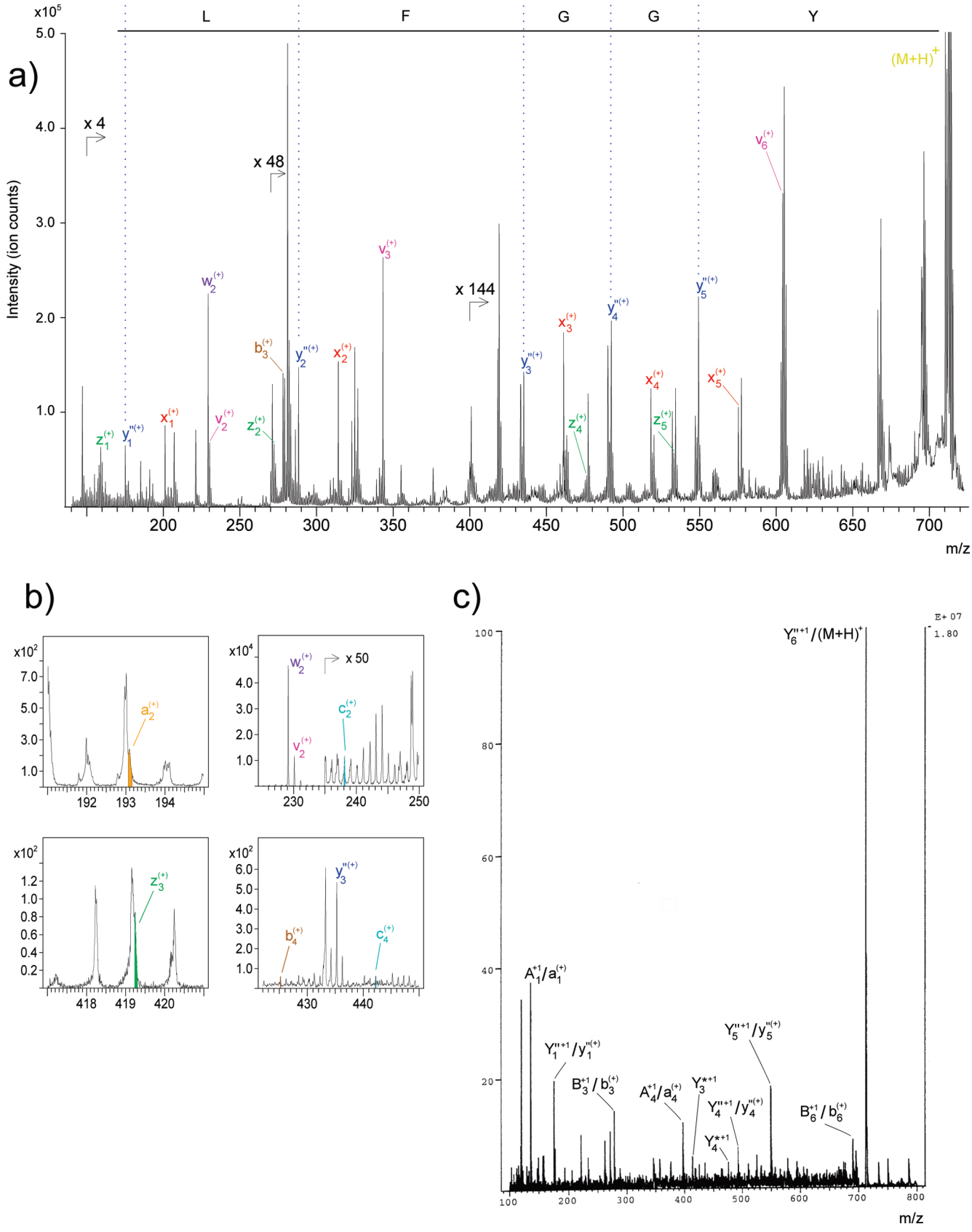

Figure 5. (a) Positive ion spectrum of DA 1−6 (YGGFLR), showing the observed backbone cleavage fragment ions labeled in different colors depending on the ion type. The upper bar shows the peptide sequence, indicating how the successive separations between sequential $y_n''^{(+)}$ peaks are used to obtain sequence information. (b) Magnified areas of the spectrum in part a, showing examples of low-yield backbone fragment ion peaks. (c) Experimental CID spectrum for DA 1−6 recorded using an ESI-MS spectrometer. The figure has been adapted from Sandin et al.[52] with permission of Elsevier. In the figure, fragment ions were originally assigned according to Roepstorff and Fohlman nomenclature. The Biemann nomenclature has been added for mere comparative purposes only.

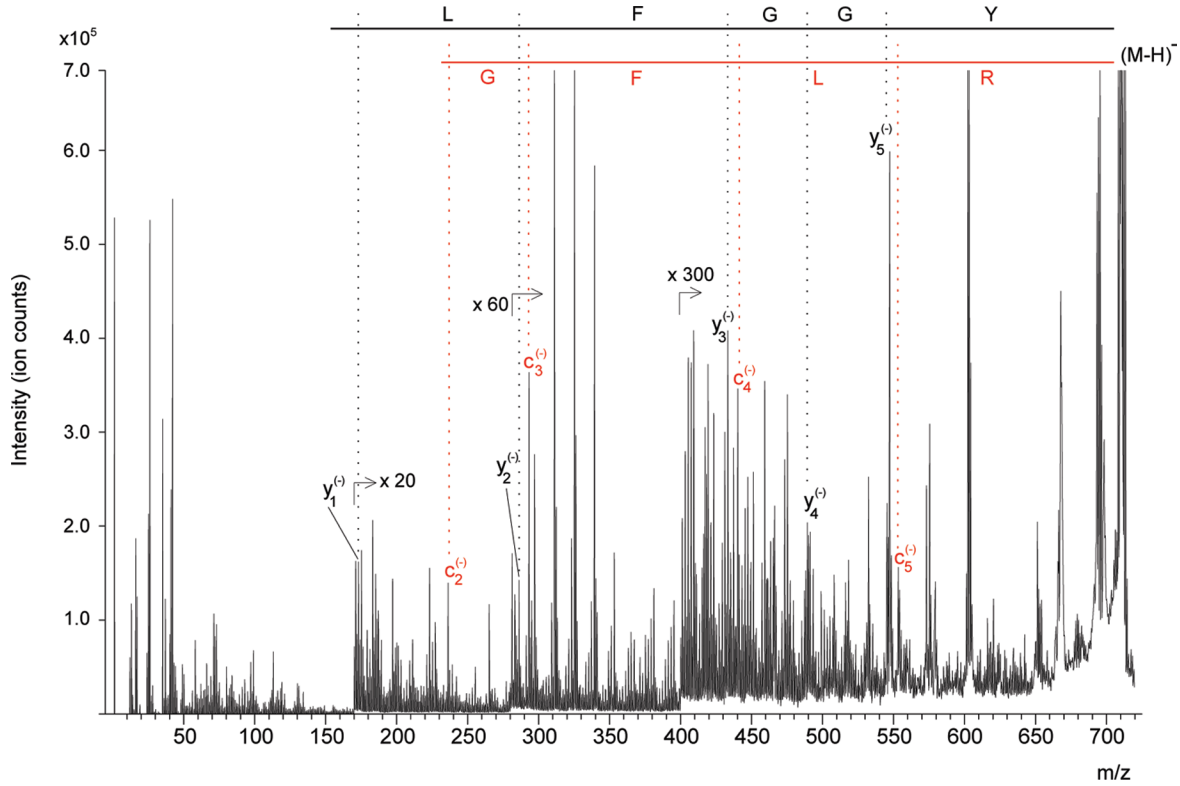

Figure 6. Negative ion spectra and sequence for dynorphin A 1−6 (YGGFLR). The upper bar shows the peptide sequence and refers to the molecular mass of $y_n^{(-)}$ ions, whereas the lower bar scheme refers to $c_n^{(-)}$ ions.

possible. DA 1−6 contains six amino acid residues, and therefore five different C−N cleavages are possible, one at each C−N bond of the peptide backbone. From cleavage of each C−N bond, different $y_n''^{(+)}$ ion fragments are formed, and adjacent ions of the same type (e.g., $y_1''^{(+)}$ and $y_2''^{(+)}$) differ by the mass of the specific amino acid residue that has been cleaved (for example, the decrease in 147.07 Da between two consecutive ions, $y_1''^{(+)}$ and $y_2''^{(+)}$, indicates that the amino acid lost between these ions is F). By using the observed backbone cleavage ions, all single amino acid residues that have been cleaved at every ion transition can be identified, and therefore, the peptide sequence can be elucidated. In this case, the sequence is shown from C- to N-terminal side. Figure 5b shows several magnified areas of the DA 1−6 spectrum. A number of N-terminal ions require magnification in order to be observed. In certain rare cases, some peaks overlap with other adjacent peaks, hindering the assignment process (e.g., $a_2^{(+)}$ and $z_3^{(+)}$ in the figure).

Figure 5c shows a previously published experimental spectrum obtained from the analysis of DA 1−6 using an ESI-MS spectrometer.[52] A number of $y_n''^{(+)}$ ions can be observed in the spectrum, together with several $a_n^{(+)}$ and $b_n^{(+)}$ ions, in good agreement with the observed ToF-SIMS spectrum in Figure 5a,b. Note that Sandin et al. have assigned the $a_1^{(+)}$ ion in the DA 1−6 spectrum. We doubt whether formation of a_1, b_1, or c_1 ions would be favored in ToF-SIMS. Unless the N-terminus is modified, it is not possible to form b_1 and c_1 ions.[53] In addition, studies on dipeptides show that, at low energies, formation of y_1 and loss of CO are favored processes over formation of a_1 ions.[54] For ToF-SIMS, we expect a fragmentation dynamics similar to low-energy CID and therefore we have not included a_1 ions in the present study.

Considering the secondary ion yields of the peaks assigned to positive backbone cleavage ions, a number of interesting observations were made (see diagrams in Figure S1, Supporting Information). First of all, there is a general decrease in the yields with increasing fragment mass. It was also found that ions holding the charge at the C-terminal side of the peptide dominate the spectra for the peptides that contain R at their C-terminal side, i.e., DA 1−6, DA 1−9, and, to a minor extent, DA 1−10. Furthermore, ions arising from cleavage of the amino acid side chain are the most intense, when formed. In contrast, for LE, which does not contain R or any other basic amino acid residue at any of the peptide sides, the spectrum is dominated by the ions that hold the positive charge at the N-terminal side of the peptide, and no side chain cleavage ions were observed. For MEKK, there is no special prevalence of any type of ions in the spectra. Note that MEKK contains K at the C-terminal side, a residue with a less basic nature than R.[54]

Similar observations have been made for CID. Due to their nucleophilic nature, basic amino acid residues attract positive charges and increase their localization.[36] Generally, for CID processes, the presence of basic residues such as R at one side of the peptide structure favors formation of ion fragments containing the charge at that specific side.[36,45,54] This effect is seen for all R-containing peptides, but not for MEKK containing

(52) Sandin, J.; Tan-No, K.; Kasakov, L.; Nylander, I.; Winter, A.; Silberring, J.; Terenius, L. *Peptides* **1997**, *18*, 949–956.
(53) Paizs, B.; Suhai, S. *Mass Spectrom. Rev.* **2005**, *24*, 508–548.
(54) van Dongen, W. D.; Ruijters, H. F.; Luinge, H. J.; Heerma, W.; Haverkamp, J. *J. Mass Spectrom.* **1996**, *31*, 1156–1162.

K. On the other hand, the spectrum for LE is similar to the spectrum of methionine-enkephalin typically obtained by CID.[36]

Finally, the ToF-SIMS spectra can be used to distinguish between the amino acids L and isoleucine (I), two structural isomers with identical molecular weight, in the DA 1−9 spectrum. Fragmentation of the side chain of I gives rise to two different fragments (w and w′) corresponding to two different substituents in the side chain ($-CH_3$ and $-CH_2CH_3$), whereas L gives only one fragment (w), since its side chain contains only one substituent. Detection of w and w′ fragments in the DA 1−9 spectrum indicates that I is contained in the sequence.

Figure 6 shows an example of a negative ion spectrum (DA 1−6) containing peaks corresponding to backbone cleavage fragments. Here, the $y_n^{(-)}$ and $c_n^{(-)}$ ions show higher intensities than all other backbone cleavage ions. As indicated in Figure 6, the observation of these ions in the spectra can be used to elucidate the peptide sequence starting either at the N-terminal side ($c_n^{(-)}$ ions) or at the C-terminal side ($y_n^{(-)}$ ions) of the peptide.

Comparing the secondary ion yields of the negative backbone fragment ions for all the analyzed peptides, the $y_n^{(-)}$ ions are the most frequently observed ions (always showing complete ion series), followed by $c_n^{(-)}$ ions (see diagrams in Figure S2 in Supporting Information). The $c_n^{(-)}$ ions seem to increase their abundance with increasing peptide lengths and have higher intensities than any other ion, when formed. Also in high-energy CID processes, the $y_n^{(-)}$ ions have been found to be the most abundant ones and they were also shown to be thermodynamically favored for CID.[55] On the other hand, $c_n^{(-)}$ ions are not specially favored in DA 1−10 spectra compared with all other peptides, suggesting no major effect of proline (P) in terms of favoring $c_n^{(-)}$ ion formation, contrary to previous CID findings.[44]

CONCLUSIONS

The results from this work demonstrate that ToF-SIMS can be used to provide a variety of useful information in peptide and protein analysis, such as information about the amino acid composition, molecular weight, and amino acid sequence. At the current stage and considering the advantages of ToF-SIMS, including the small sample amounts needed for analysis, the ease of sample preparation, and the capability to image the spatial distribution in, for example, tissue samples, the method may be a valuable complement to MALDI and ESI in protein and peptide analysis. In proteomics, we think ToF-SIMS will be especially useful in applications where low sample amounts are a limiting factor and where imaging and/or molecular microanalysis would provide new opportunities, such as in miniaturized analysis platforms (arrays, microfluidics, etc.) and in the analysis of native biological structures in cells and tissues. With respect to biological samples, the chemical complexity puts severe limitations to the detail of information that can be accessed, e.g., the amino acid sequence is most likely possible to obtain only from pure peptide samples or mixtures of a few peptides. However, this chemical complexity can in many cases be reduced by the capability of ToF-SIMS to specifically analyze (spatially separated) small structures.

The analysis of opioid and amyloid β peptides in this work reveals important similarities between ToF-SIMS and CID. These similarities are, to some extent, expected, considering the present understanding of the sputtering process using cluster projectiles.[56] The high energy of the incident primary ion is expected to rapidly dissipate through multiple collision processes in the surface region, resulting in a large number of low-energy collisions (eV range), causing intact particle ejection and softer fragmentation events. For these processes, it is likely that a fragmentation dynamics similar to low-energy CID takes place. Low energy collisional activation involves primarily vibrational excitation, leading to lower fragmentation and a wealth of ions being formed, similar to what has been seen in the ToF-SIMS spectra of peptides.

In addition to information about the amino acid composition, molecular weight, and detection limits, we have demonstrated the capability of ToF-SIMS to provide amino acid sequence information, by observation of a series of multiple amino acid fragment ions. The abundance of these ions shows large variations which, however, follow similar trends as in CID.

(55) Bowie, J. H.; Brinkworth, C. S.; Dua, S. *Mass Spectrom. Rev.* **2002**, *21*, 87–107.
(56) Delcorte, A.; Bertrand, P.; Garrison, B. J. *Appl. Surf. Sci.* **2003**, *203*, 166–169.

ACKNOWLEDGMENT

This research was supported by EC FP6 funding (contract no. 005045 NANOBIOMAPS), Swedish Governmental Agency for Innovation Systems (VINNOVA), Swedish Research Council (VR), Fundació la Marató de TV3, and Stockholm County Council. The authors thank Birgit Hagenhoff and Selim Sengul for helpful advice.

SUPPORTING INFORMATION AVAILABLE

Figures S1 and S2. This material is available free of charge via the Internet at http://pubs.acs.org.

Received for review November 27, 2009. Accepted January 12, 2010.

AC902712F